

Improvements in LED-based fluorescence analysis systems

Andrew E. Moe, Steve Marx, Naureen Banani, Matthew Liu,
Brian Marquardt, Denise M. Wilson*

Department of Electrical Engineering, University of Washington, Seattle, WA 98195-2500, USA

Received 24 September 2004; received in revised form 28 January 2005; accepted 31 January 2005

Available online 27 April 2005

Abstract

This paper presents results from an electronic interface that significantly improves the stability, power output, and spectral flexibility of light emitting diode (LED)-based systems used to excite fluorescence or other forms of luminescence. LEDs are an attractive alternative to conventional white-light sources used in fluorescence analysis because of reduced power of operation, enhanced modularity, reduced optical loss, fewer imaging artifacts, and increased flexibility in spectral control without the need for high overhead optics. Drawbacks of previously presented LED-based systems include insufficient light output, instability (poor lifetime), and limited flexibility in broadband spectral output. The LED-array-based system here presents, up to a 93% improvement in stability over other LED-based systems, up to 100-fold increase in light output over single LED systems, and millions of possible combinations of spectral output (as compared to a 1–10 possible spectral outputs with one to two LED array-based systems). These benefits over previous LED-based systems are achieved at a reduction in power, space, and cost of at least one order of magnitude over conventional white-light source-based systems. Used in conjunction with appropriate optics, this electronic interface provides a highly competitive, portable (small footprint) alternative to conventional fluorometer designs. © 2005 Published by Elsevier B.V.

Keywords: Fluorescence; Luminescence; LED; Biomedical instrumentation; Electronic interface

1. Introduction

Traditional fluorescence analysis systems (used in most benchtop fluorometers) use a high-power white-light source chosen for high power output and broadband spectral output. For example, a typical xenon lamp produces 150 W of output power in a uniform band from 300 to 800 nm (Fig. 1a). Unfortunately, xenon lamps also require high current power supplies (25 A and 20–40 kV to initiate an arc) [1] and special handling. Xenon lamps operate under very high pressure (usually around 10 atm), which also creates an explosion hazard. Gloves and safety glasses are always required when handling, both to protect the user and the bulb. The bulb cannot be touched with a bare hand; the resulting fingerprint will char and possibly cause the bulb to explode. The high voltages required to start the arc can also interfere with nearby electron-

ics. Since the xenon lamp uses an arc to generate light, images of the arc (called artifacts) are often projected onto the sample under analysis, which hinders the uniformity of the excitation, and therefore, the (spatial) reliability and consistency of the output (emission) signal. Another common alternative, the mercury (Hg) lamp produces strong spectral lines across a wide range of wavelengths. These lines occur at narrow bands of wavelengths from 250 to 600 nm (Fig. 1a), which make them useful for fluorescence instrumentation only if the fluorophore absorption spectrum is compatible with lamp's spectral lines. Mercury lamps, like their xenon counterparts, also require high power supply voltages and special handling. Mercury arc lamps create mercury vapor in the lamp, which when released, is extremely toxic. Imaging artifacts also impact the spatial uniformity of the excitation signal delivered to the sample under analysis. Despite these drawbacks, however, high-powered white-light sources remain a desirable design choice for fluorescence analysis systems because of their uniform broadband and high power output. Uniform broadband

* Corresponding author. Tel.: +1 206 221 5238; fax: +1 206 543 3842.
E-mail address: denisew@u.washington.edu (D.M. Wilson).

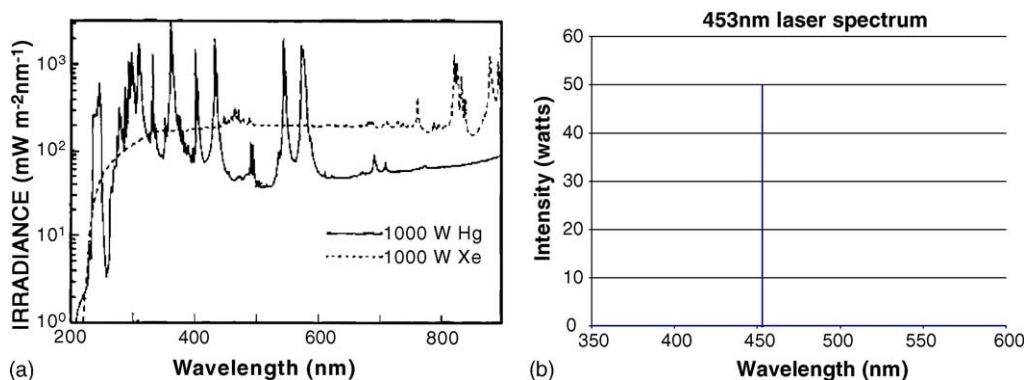


Fig. 1. Conventional light source spectra for fluorescence analysis systems. Shown are the output spectra produced by: (a) [1] xenon and mercury lamps and (b) an argon-ion laser, common choices for exciting fluorescence in biological analysis applications. Broadband light sources incur high optical losses but are suitable for general-purpose use, while lasers incur lower optical losses at the expense of limited application.

characteristics are desirable for general-purpose instrumentation. In a typical fluorometer, the input light power from a white-light source, is transferred through a monochromator, where only a small spectral band (1.5–20 nm wide) is focused and retained for excitation of the fluorescence sample. This approach is often thought to be most appropriate for general-purpose instrumentation, because, from a uniform broadband spectrum (relatively constant over wavelength), a large selection of small spectral bands of similar output power is available. The user can easily change spectral bands, by adjusting the monochromator settings. Unfortunately, most of the input power is lost in the spectral filtering. All light power that is not in the (narrow) desired wavelength band is filtered out of the signal used to excite the sample under analysis.

Lasers are another viable choice for fluorescence excitation. A laser produces high-power light within a narrow spectral band (monochromatic, Fig. 1b), thereby eliminating the need for an external monochromator and optical filtering, but limiting the flexibility of the laser excitation to fluorophores that respond efficiently to the laser's excitation band. Lasers also require high power supply voltages, consume a great deal of power, and are often quite expensive.

LEDs are an attractive alternative to conventional white-light sources and lasers used in fluorescence analysis because of reduced power of operation, fewer imaging artifacts, and increased flexibility in spectral control without the need for high overhead optics. LEDs, at a systems level, consume less power, because less light is wasted in the filtering process that occurs between the input light source and the sample itself. The reduction or absence of optical filtering in the excitation path is a direct result of the fact that the spectral output of these devices is more narrow than that of white-light sources (Fig. 2a). When the type of LED is chosen appropriately, the spectral characteristics can match the fluorescence efficiency of the sample under analysis reasonably well (Fig. 2b), thereby reducing the need for optical filtering (through a monochromator or conventional optical filter). Since LEDs produce no arc and contain no filament, they produce no artifacts on the sample; LEDs are also sufficiently

small that they can be easily interchanged in a fluorescence analysis instrument, thereby enabling spectral flexibility in the control of the light source without incurring a need for additional optics. Low cost, low power, high uniformity, and high modularity make LEDs desirable in many fluorescence analysis tasks.

LEDs have been used in a variety of research efforts and commercially available systems as alternatives to higher powered light sources, such as lasers and xenon (broadband) lamps. Blue LEDs have been used in a variety of research efforts [5–7] because of the compatibility between the blue LED emission spectrum (peak wavelength between 450 and 500 nm) and the absorption of many common fluorophores. For example, Dets and Denisov [5] use a single blue LED, in conjunction with fiber optics, to analyze biopsy samples from the gastrointestinal tract. Results from this battery powered, hand-held system are benchmarked against those using a conventional (He–Cd) laser system, which produce comparable spectral output but suffer from inferior power output (and signal-to-noise) characteristics. Likewise, Liew et al. [6] compare the results of a blue LED (475 nm peak emission), tungsten–halogen lamp, and laser (532 nm peak emission) for analyzing green fluorescent protein (EGFP) tagged to antibody resistance agents in monitoring the safety of genetically modified plants. Of the three light sources under analysis, the LED and laser are best matched to the absorption characteristics of the fluorophore, providing the (highest) optical output after appropriate filtering. Other research efforts have similarly demonstrated the viability of green [8,9] and purple [10] LEDs for fluorescence intensity measurements as well as green [11] and UV LEDs [12,13] for fluorescence lifetime measurements. Arrays of LEDs, whereby single LEDs are used in turn, have also been demonstrated for fluorescence lifetime measurements [14] and monitoring of thermal cycling in DNA analysis [15]. Commercially available systems, such as those produced by Ocean Optics [16] and Turner Biosystems [17] reflect the popularity of the LED for portable instrument use. The Ocean Optics USB-LS-450 module [16] uses a blue LED in conjunction with a USB2000

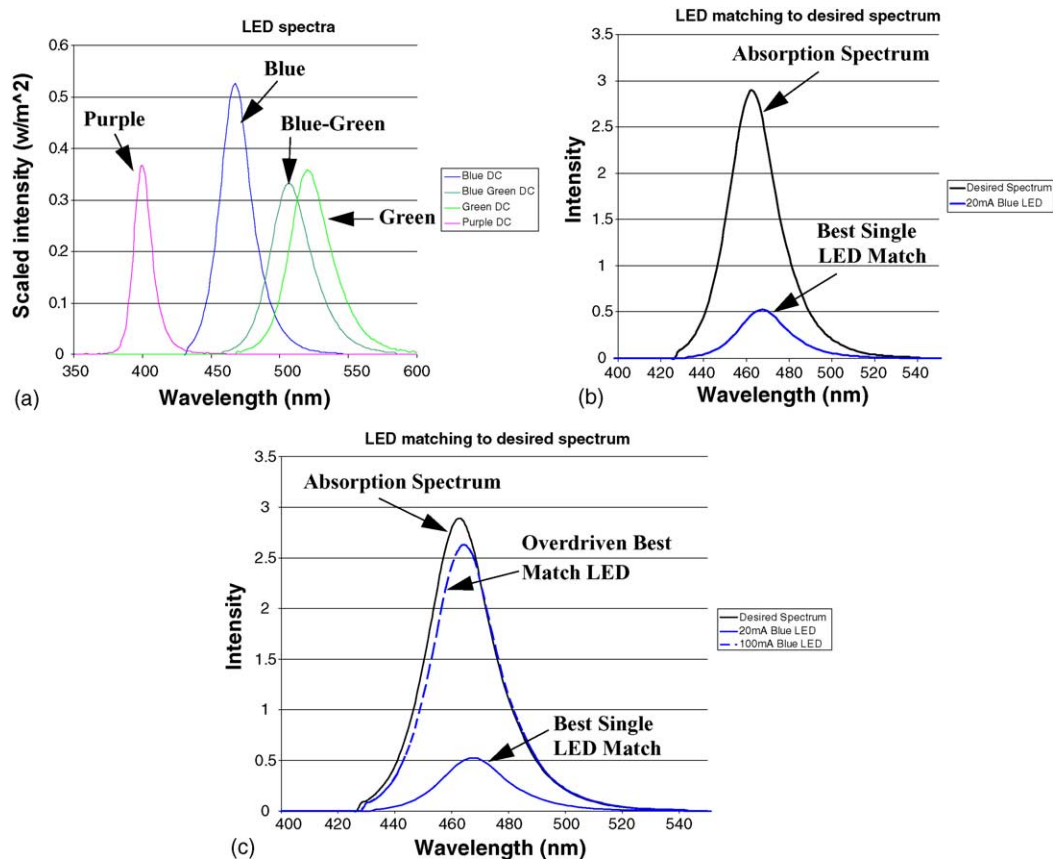


Fig. 2. LED light source spectra for fluorescence analysis systems: (a) commercially available LEDs provide a wide variety of moderately broadband spectra, which can be (b) best-matched to fluorescence absorption (efficiency) spectra; (c) overdriving these LEDs not only generates increased optical power output, but also generates small spectral shifts that can be used to improve the match between the excitation source and absorption spectrum of the fluorophore.

spectrometer for general-purpose fluorescence analysis. An SMA connector for use with fiber optics and a built-in collimating lens make this an easy module to insert into a fiber optic-based optical testbed. Turner Biosystems [17] produces a similar portable system using one to two LEDs for excitation. Both in the research and the commercial arenas, LEDs have demonstrated widespread use and popularity for fluorescence analysis systems, primarily for portable instrument use (lower cost, power, size, or weight).

In these and other research and commercial systems, LEDs are typically operated under nominal, manufacturer-recommended conditions, in order to maintain the lifetime stability of the LED within reasonable limits for biological experimentation and instrument maintenance intervals. Under these conditions, the (light) power output of the input source rarely exceeds 50 mW per LED, which is often insufficient to induce measurable fluorescence (emission) in many low concentration applications. In addition, the spectral output of the LED is constant under nominal conditions and even under “best-match” conditions, it may be limited in its ability to meet the best absorption efficiency of the fluorescence sample under analysis.

Increased light power output and spectral flexibility can be achieved by overdriving LEDs, where the current through

the LED exceeds the nominal operating current up to an order of magnitude. Driving high currents through an LED accomplishes two objectives (a) increased light power output that scales linearly with the input (electrical) power and (b) fine (small) spectral shifts toward the blue (shorter) wavelengths (Fig. 3b). Overdriving LEDs at higher currents, however, often results in prohibitively low lifetimes of the LEDs. Using an array of LEDs, driven at a variety of nominal and overdrive operating conditions, can result in a wide range of power outputs as well as an immense number of possible spectral outputs that can be “best-matched” to the absorption efficiency of the sample under analysis. Details regarding the automated optimization of instrument design using these types of LED arrays are described elsewhere [18]. Lifetime limitations associated with overdriving LEDs can be overcome by reducing the percentage of time, over a signal acquisition cycle, during which high current flows through the LED. This paper presents an electronic system interface that enables higher drive currents (and higher light intensity levels) of standard LEDs while extending their lifetime through significantly reduced duty cycle operation. Experimental results show stable operation at a wide range of duty cycles and current levels, and fine (small) spectral shifts with increasing current levels for a variety of LEDs. LEDs operating under such conditions

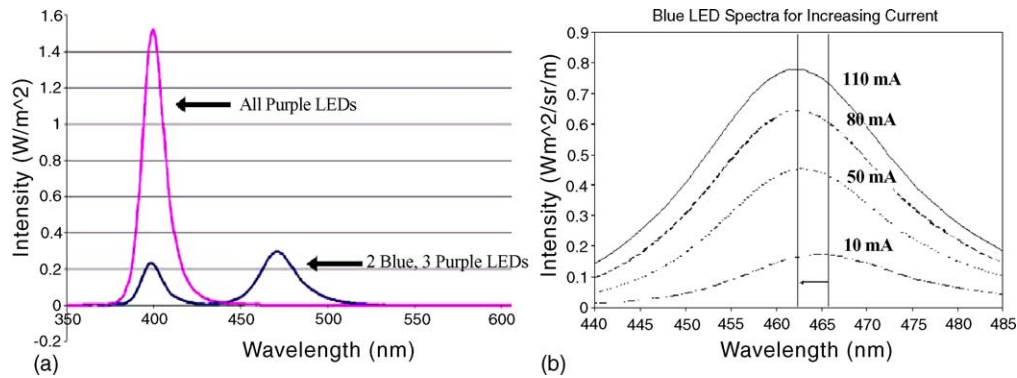


Fig. 3. LED system experimental results: spectral variability. Shown are representative results from the two types of tuning available in the LED-based system: (a) coarse tuning available through changing the type of LEDs in the array; (b) fine tuning (small spectral shifts toward shorter wavelengths) available by overdriving the LEDs at high currents.

have shown comparable performance to white-light sources (e.g. xenon) in representative applications (detecting fluorescence intensity in Rhodamine dye and GFPuv-stained AM1 *Methylobacterium extroquens* bacteria).

2. System description

The LED array module is designed to be incorporated into a general-purpose fluorescence analysis system that enables comparable or improved performance to many existing white-light source-based fluorimeters within a smaller cost, size, and power footprint. The miniaturized system design is shown compared to a conventional design in Fig. 4.

Conventional systems (Fig. 4a), designed for general-purpose fluorescence analysis typically consist of a broadband light source (e.g. xenon or mercury lamp) that produces a broad spectral output within the visible light wavelengths. The light is then filtered, using a monochromator that typically transfers a user-selected 1–20 nm band of light, blocking on the order of 95% of the excitation light that reaches the sample under analysis. Conventional, discrete optics then collimate and transfer the light to the sample, which absorbs a percentage of the incoming light (according to Beer's law and

the absorption spectrum of the fluorophore), emitting light, whose total power content is significantly reduced from the input power. The emission signal is then transferred through other discrete optical filters and lenses, until it is collected by a high precision photodetector (e.g. photomultiplier tube) at the end of the signal path. Optical power loss in these conventional systems is dominated by optical and filtering losses at the input monochromator. As a result, in conventional fluorescence analysis systems, the consumption of optical power is highly inefficient in order to preserve the general purpose and tunable nature of these systems.

The LED-based fluorescence analysis system architecture (Fig. 4b), on the other hand, consists of an array of up to seven LEDs (e.g. blue, purple, and green) that produce a narrow band of spectral output within the visible light wavelengths. The selection of the LEDs, and related spectral output, is optimized to the absorption characteristics of the fluorophore(s) under analysis using a software simulation platform described elsewhere [18]. As a result, a monochromator is not required in the optical path between the input light source (LED array) and the sample under analysis. Randomizing fiber optics combine the outputs of the LED array into a single aggregate output that is both uniform (homogeneous spectral characteristics) and absent of imaging artifacts (com-

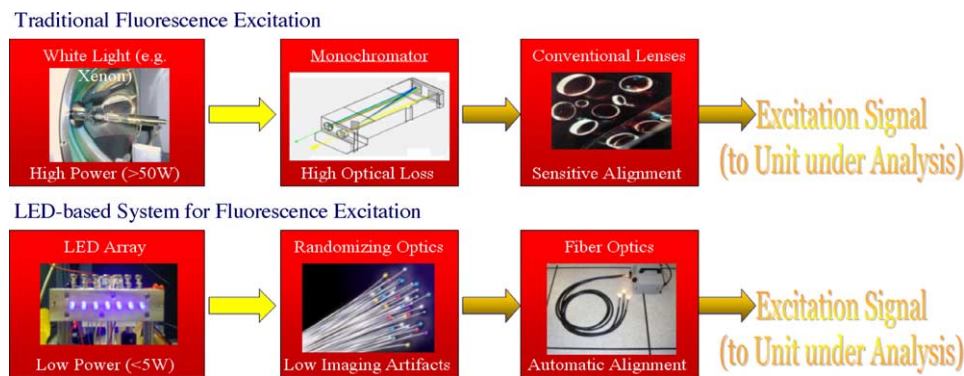


Fig. 4. Conventional white-light excitation sources vs. LED-array-based source: (a) conventional excitation systems employ high-power light sources with monochromatic emission spectrum selection. Discrete optics require sensitive alignment and ambient light isolation. (b) LED-based excitation uses fiber optics to eliminate alignment and ambient light issues, while aggregating LEDs driven to a tuned spectrum into a single source for excitation.

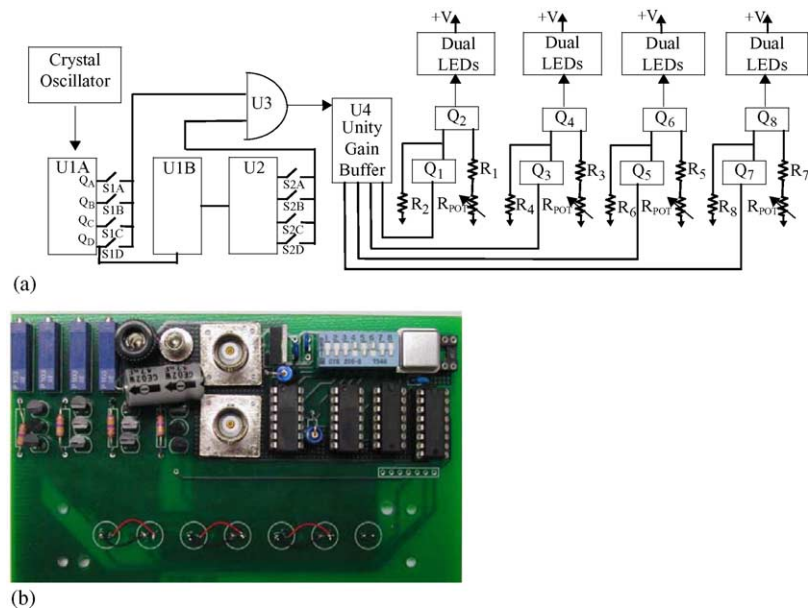


Fig. 5. LED-array electronic interface shown are: (a) schematic and (b) discrete implementation of the LED interface. The electronic interface enables automated or manual control of the current and duty cycle to which the LED is driven. A low duty cycle pulse generated by the onboard oscillator (upper left of schematic) drives the high current LED driver circuits (upper right of schematic). Current supplied by each driver circuit is adjusted with the potentiometers in the upper left of the PCB.

mon with arc and filament-based systems). The output of the randomizing optics is transferred to the sample under analysis and its fluorescence emission is monitored using a similar optical path to the conventional system. Ongoing work includes the placement of feedback loops in the input and output optical paths to control the stability of the LED array and monitor the spectral output of the fluorescence emission (output) signal, respectively. Intensity degradation and wavelength instability can be monitored and compensated for in this system, allowing maximum LED lifetime and consistent, repeatable spectral output for a miniaturized fluorescence analysis system. All optics in the LED-based system architecture are based on fiber optics, which inherently produce less optical loss than conventional discrete optics in the signal path. In this way, the LED array is able to excite fluorescence at a much lower input power using fewer optical filters (monochromators) and losses. Furthermore, conventional systems require sensitive alignment of discrete optics, and must be enclosed to prevent ambient light from entering the system. Using fiber optics enables easier (automatic) alignment and improved modularity in the LED-based system.

3. Electronic interface circuit description

The schematic and PCB-level implementation of the LED driver module is shown in Fig. 5. Using this interface, the LEDs can be driven at a range of duty cycles and frequencies. Current through four pairs of LEDs can be controlled independently, for a total possible array size of 8. The de-

sign is modular to enable easy expansion of the array size. The electronic interface consists of two major circuits: (a) an analog high current driver and (b) a digital oscillator. The high current driver enables the current through the LEDs to be adjusted up to 350 mA. The digital oscillator enables control pulses ranging from 0.39 to 25% duty cycle and frequencies ranging from 23.44 to 187.5 kHz.

The digital oscillator consists of a crystal oscillator, several counter circuits, and a buffer. The 74393 counter IC (U1A, U1B, U2) divides the input by 2 (QA), 4 (QB), 8 (QC) or 16 (QD). The first counter (U1A) is driven by the crystal oscillator chosen at 6 MHz for this implementation. The frequencies of the output of U1A are, therefore, 3, 1.5 MHz, 750, and 375 kHz. The low frequency output (QD) of U1A is used as the frequency input to U1B, producing a division of the original 6 MHz input frequency by 32, 64, 128, and 256 at the output of U1B. These four frequencies (187.5, 93.75, 46.875, and 23.44 kHz) are selected using the switch S1 which can either be manually or electronically controllable; in this case, a manual DIP switch is used to select from the four frequencies. The second switch S2 selects from the output signals of U1A (3, 1.5 MHz, 750, and 375 kHz). The signal selected by S1 is transferred to an AND gate (U3), where it is combined from the signal from S2 to produce an LED control signal of duty cycles ranging from 0.39 to 25% and frequencies ranging from 23.44 to 187.5 kHz. The 16 possible frequency/duty cycle pairs are noted, according to switch settings in Table 1. The driving (control) signal is then buffered by the unity gain buffer U4 and transferred to transistors Q_1 , Q_3 , Q_5 , and Q_7 for alternately enabling and disabling the LEDs at the desired duty cycle and frequency.

Table 1
Duty cycle setpoints for the LED drive electronics

	Pulse width (S2)	Switch 5	Switch 6	Switch 7	Switch 8
Period (S1)	Multiplier	32	64	128	256
Switch 1	1	3.1%	1.6%	0.78%	0.39%
Switch 2	2	6.3%	3.1%	1.6%	0.78%
Switch 3	4	12.5%	6.3%	3.1%	1.6%
Switch 4	8	25%	12.5%	6.3%	3.1%

The high current analog circuits are driven by the control signal from the digital oscillator circuit as just described. To conserve space, the current for each (parallel) pair (rather than each individual LED) is controlled by a combination of two BJTs, two resistors and a 20 Ω potentiometer. Operation in each of the four stages (controlling two LEDs per stage) is identical. Consider the operation of the first stage controlled by Q_1 , Q_2 , R_1 , R_2 , and R_{POT} . Transistor Q_1 is driven by the oscillating output from the buffer U4 in the digital oscillator circuit. When the base of Q_1 is a logic high, maximum current flows through each of the first two LEDs:

$$I = \frac{(V_{in} - 1.4)}{2R_{POT}} \quad (1)$$

The variable resistor R_{POT} allows direct manipulation of the current supplied to the LEDs (I). The small series resistance R_1 is provided to set the maximum current for the system. When R_{POT} is set to zero, the combined series resistance will be equal to R_1 resulting in maximum current flow. The LED driver includes a TTL synchronization output for connection to other devices. For example, a photodetector in the output optical path can be synchronized to the LED driver, using this signal, so that the photodetector output is only computed and processed, when the LEDs are on.

4. Experimental setup

The interface for the LED array is tested both in a circuit and a systems context. Circuit testing is done simply by driving the LED array at its 16 possible duty cycle setpoints and monitoring the voltage across a 1 Ω resistor connected in series with any individual LED. The voltage (which is equal to the current) is monitored using a Tektronix TDS7104 oscilloscope and the duty cycle and frequency monitored using a Hewlett Packard 53131A counter; rms variations in the duty cycle and LED current are computed from data collected by the counter and the oscilloscope, respectively. Results from circuit level testing are described in detail in Section 5.

The interface is tested in a system context using a modular testbed in our laboratory (Fig. 4). It consists of the LED driver interface, LED array, fiber optic coupling in the excitation and emission path, a (sample) cuvette, and a dual output path that enables simultaneous connections to a spectrometer and a photodetector for fluorescence signal collection and analysis. The testbed is highly modular to enable quick and efficient replacement of LEDs, photodetector, and sample.

The LED driver interface can control up to seven LEDs at one time. These seven LEDs are mounted in a secure coupler that efficiently couples the LED light output to a fiber optic output. The coupler consists of four layers. The first layer securely holds the LEDs; the second layer places ball lenses in the optical path to collimate the light for maximum coupling; the third layer provides inserts for optical filters (optional); and the fourth layer consists of SMA bulkheads that provide the final connection between the LED array and a randomizing fiber optic bundle which aggregates the seven LED outputs into a single uniform beam of light.

Output light from the sample is transferred to another fiber-optic path into an Optometrics DMC1-03 mini-monochromator, which enables narrow filtering of light for system characterization and analysis. Filtering levels are chosen to minimize the excitation light that is transferred or bleeds-through into the emission signal. A second optical beam splitter then transfers the filtered emission signal to: (a) a modular photodetector holder capable of accommodating a range of commercial photodetectors as well as custom photodiode arrays and (b) another Ocean Optics HR2000 spectrometer for spectral analysis and verification. The light output of the LED driver interface is characterized in this testbed under no sample (empty cuvette) conditions.

In addition to demonstrating performance in the testbed described above, the LED array module (LED driver interface, LED array, coupler, and randomizing fiber optics) has been used to replace the input light source in a conventional fluorometer (Shimadzu RF3401 PC) to benchmark performance of the LED module with a conventional xenon light source in gathering emission from GFPuv (ultraviolet green fluorescent protein) tagged to AM1 *M. extroquens* bacteria and Rhodamine 123 dye. Absorption and emission characteristics for GFPuv fluorescing agents can be found in references [19,20], respectively. Results of system level testing are described in detail in Section 6.

5. LED electronic interface: results and discussion

The LED driver is controlled by a series of switches (either manual or electronic) over which a total of 16 possible duty cycles and variable drive currents from 20 to 350 mA can be selected. The drive current range covers a spectral shift of approximately 16 nm for the typical LED between nominal current and maximum current operating conditions; the peak wavelength and spectral shift from nominal operating conditions for a range of commercially available LEDs, characterized for fluorescence analysis, are shown in Table 2.

In this implementation, the LEDs are controlled in pairs to conserve space; however, it is possible to control both the duty cycle and the current through each LED separately by dedicating a driver circuit to each LED. The relationship between the switch settings and corresponding duty cycle/drive current settings is described in Table 1. Typical behavior of the LED driver electronics is shown in Fig. 6, for several

Table 2
Spectral behavior of representative commercial LEDs for various operating conditions

LED specifications				Spectral shift			
Color	Supplier	Part #	Peak, λ (nm)	20 mA (nm)	50 mA (nm)	80 mA (nm)	100 mA (nm)
Purple	www.ledsupply.com	L4-1-U5TH15-1	395	0	+1	+2	+5
Blue	www.ledsupply.com	L1-0-B5TH30-1	469	0	-2	-3	-4
Blue-green	www.ledsupply.com	L4-0-T5TH30-1	508	0	-3	-4	-5
Green	www.ledsupply.com	L1-0-G5TH30-1	521	0	-3	-4	-5

different discrete settings of the switch-based controls. For a setting, where switches 4 (S1) and 5 (S2) are active, the driving (control) pulse to all LEDs is a TTL signal of frequency 375 kHz and a duty cycle of 25% (e.g. the signal is active high for 25% of the total period). Similar square wave behavior is obtained across the full range of LED settings from low currents and low duty cycles to high currents and high duty cycles.

The circuit parameters most relevant to fluorescence analysis to using LEDs as a light source are:

Current noise (A): Noise in the drive current for the LEDs, while the LED is above threshold (“on”) is translated directly to noise in the LED optical output power and is transmitted through the optical path to the photodetection stage. On the other hand, noise that occurs, while the LED is below threshold (“off”) does not affect the LED optical output power at all (since the LED is off) and is not transmitted through the optical path.

Duty cycle noise or “jitter” (%): Fluctuations in the duty cycle of the LED due to noise in the digital oscillator circuit are translated directly to fluctuations in the duty cycle of the LED optical output power and are transmitted through

the optical path of the analysis system to the photodetection stage.

Stability in LED optical output power (W/h): Since the LEDs are driven at currents up to 20 times their nominal (manufacturer-recommended) values, their performance (optical power output) will degrade more quickly over time with increasing drive current.

Response time (ns): The time between the rise of the driving (control) signal from the digital oscillator circuit and resulting peak optical power emitted from the LED is a delay that impacts the accuracy of the photodetection signal at the other end of the optical path.

The degree to which these parameters affect the performance of a fluorescence analysis system is highly dependent on other characteristics of the system, most notably the photodetector used to collect the emission signal at the end of the optical signal path.

The **current noise** in the LED driver module, while the LED is “on” (e.g. during the active part of the duty cycle) affects the signal-to-noise ratio at the signal collection (photodetection) stage in the signal processing path. Most photodetectors, with the possible exception of the avalanche pho-

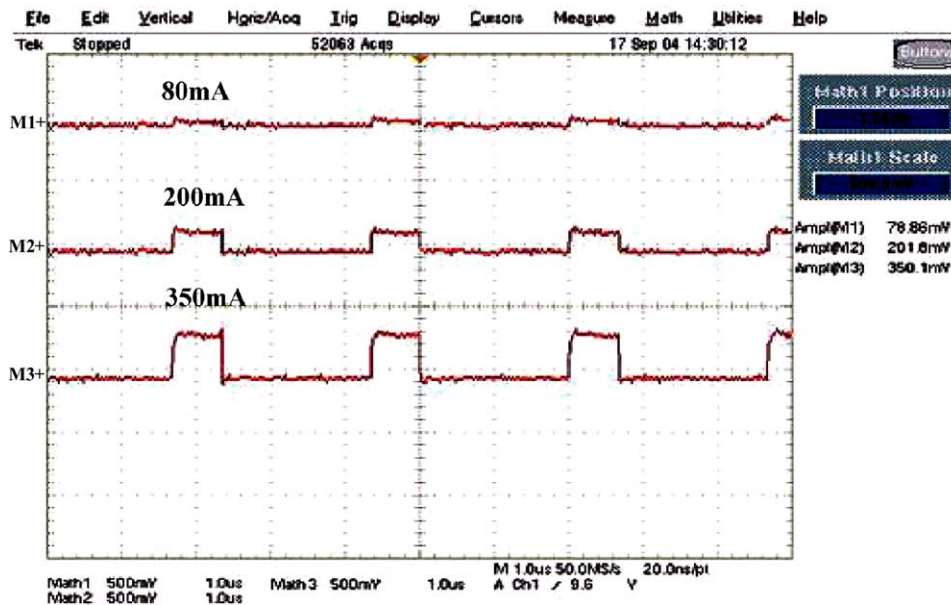


Fig. 6. LED driver interface circuit: experimental results. Representative results are shown for various drive current levels (80, 250, and 350 mA) at a duty cycle of 25%. Switches S1(4) and S2(5) are active to obtain this setpoint: 25% duty cycle and 375 kHz. Similar behavior is possible for the 15 other setpoints as described in Table 1.

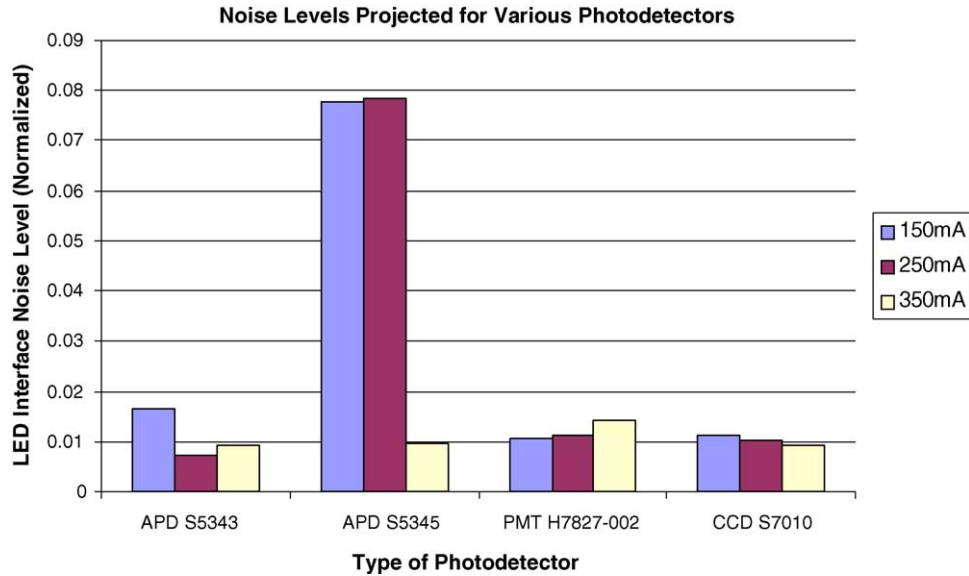


Fig. 7. Projected noise levels for common photodetectors in fluorescence analysis systems. While the noise levels in the LED drive current are relatively high (due to the use of discrete resistors and bipolar junction transistors in the discrete implementation), the “effective” noise seen at the end of the signal path will be much less due to the inherent (APD) and explicit (CCD, PMT) integration functions in the photodetectors. Results are shown for the worst-case integration times (minimum) of the various photodetectors and are normalized against the raw (no integration) noise in the controlling current for each LED.

todiode (APD), integrate input optical power to obtain an output electrical signal. The rms noise levels in the drive current are 17, 20, and 20 mA for drive currents of 150, 250, and 350 mA, respectively (taken at a frequency of 375 kHz and duty cycle of 25%). Significant improvements in these noise levels can be achieved by transistor (rather than discrete resistor) control of the LED current in a design that is based on a microprocessor for full automation of the LED module.

The impact of the noise in the LED drive current (and the emitted optical power) is then dependent on the integration time. To evaluate the effectiveness of the LED electronic interface, measured noise (LED drive current) values at various drive currents are correlated against the minimum and typical integration times for common photodetector technologies used in fluorescence analysis systems. The results are shown in Fig. 7. A typical APD for these applications (from the Hamatsu S5343–5345 series) has a cut-off frequency (f_c) between 250 MHz (S5343) and 8 MHz (S5345). Assuming that the APD measurements are taken without external integration in the measurement process, the “effective” (worst-case) noise level for the APD contributed by the LED driver circuit is calculated as the rms noise of the drive current averaged over the upper cut-off period ($1/f_c$) of the APD. For the PMT (photomultiplier tube: Hamamatsu H7827 series) and CCD (charge coupled device: Hamamatsu S7010), the signal is externally integrated over some integration time T_{int} . Integration, while slowing the measurement process, inherently reduces the noise in the final signal. Worst-case noise levels for both the PMT and the CCD are expressed as the rms noise of the LED drive current averaged over the minimum integration time for each of these devices. Noise levels are normalized to the maximum noise level (calculated at the maximum

sampling rate of the oscilloscope) in Fig. 7 for comparison among the APD, PMT, and CCD. The way in which the noise level of the LED module (and emitted optical power of each LED) correlates to the noise level in the photodetector (and resulting signal-to-noise ratio) is highly dependent on the characteristics of the sample and optical train. The efficiency with which input optical power is converted to fluorescence emission, losses in light through the optical path, noise in the sample itself, autofluorescence, and the bleed-through of excitation (LED) light to the emission path all influence the efficiency with which noise in the driving (control) LED array is coupled to noise in the photodetection (signal collection) process.

A standard approach to reducing the impact of noise (improving the signal-to-noise ratio) in fluorescence analysis systems is to integrate an optical signal for a longer time period. If such a system is coupled to the LED electronic interface and LED array described here, it is possible that the integration period of the photodetector may extend beyond the period of the LED drive signal; in this case, fluctuations (“jitter”) in the duty cycle of the LED driving pulse contribute to the overall noise in the system. “Noise” in the duty cycle of the LED driver interface for various drive currents and duty cycles is listed in Table 3. In the worst-case (at 6.3% duty cycle and high drive current), “jitter” in the drive pulse produces an SNR of 250, providing a highly stable signal to the sample under analysis and remaining signal path.

The *stability* of the LED optical power is defined as the ratio between change in LED optical power and time of operation, which directly affects the accuracy and precision of the fluorescence analysis system, when intensity measurements are used (as in fluorescence imaging or intensity-based fluo-

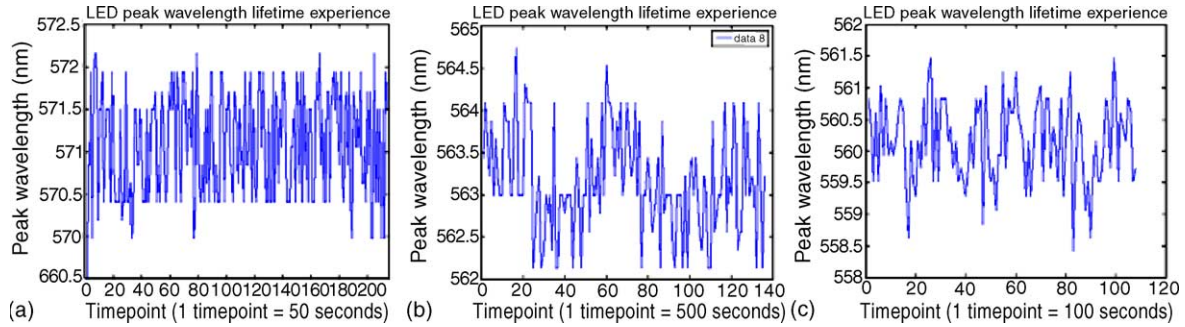


Fig. 8. LED electronic interface results: stability of optical spectral output. Shown is the spectral stability of a green LED over time for: (a) dc operation; (b) 25% duty cycle operation; (c) 1% duty cycle operation. Fluctuation in peak wavelength output varies at an rms value of 0.7 nm for each configuration, demonstrating that the electronic interface has minimal impact on the spectral stability of the LED while enabling significantly longer lifetime.

Table 3
Typical noise levels for the LED driver interface

Setpoint		rms noise	
Current (mA)	Duty cycle (%)	Current	Duty cycle (%)
250	25	20 mA	1.41E-2
	12.5	20 mA	2.29E-2
	6.3	20 mA	2.55E-2
350	25	20 mA	1.84E-2
	12.5	20 mA	4.46E-2
120	25	17 mA	1.29E-2

rophore concentration determination). In this design, elevated current levels, well beyond the manufacturer-recommended operating current, have been used to boost output optical power as well as to provide “fine” spectral shifts in the LED emission signal. Overdriving LEDs in this way limits their lifetime, and in order to preserve lifetime, reduced duty cycle operation has been integrated into the electronic interface. Various commercially available LEDs (blue, blue-green, purple, green) have been experimentally measured with varying drive currents (20, 80 mA) and duty cycles (1, 25%, and dc) to characterize their intensity lifetime and spectral stability. An example of the characterization results is shown in Figs. 7 and 8. A typical green LED is driven at 80 mA dc. Spectral data were captured with an Ocean Optics HR2000 spectrometer, with full spectral snapshot acquisitions taken every 5 s for 3 h of continuous operation. Over this short time period, the optical intensity of the LED degraded by more than 35%. Running a similar experiment, operation at a 25% duty cycle results in only 2.5% degradation over the same time period. Extending the test to 20 h of continuous operation (at 25% duty cycle) results in 4.7% degradation. Stability of the LED has increased by 93% at a 25% duty cycle. As the duty cycle is decreased further, the lifetime again increases significantly. Driving with an 80 mA and 1% duty cycle signal, the LED is shown to have no detectable degradation in the first three continuous hours of operation.

The **response time** for the PCB-based implementation of the LED driver is well suited to fluorescence intensity measurements. Maximum response time of this PCB-based im-

plementation of the LED driver circuit is on the order of 40 ns (rise time of the active pulse). To calculate the error that the finite frequency response of the LED driver circuit contributes to the collected photodetector signal, consider that a typical photodetector integrates the incoming light signal over a period T_{int} . In the worst-case, the input light source is “off” (ineffective) for the entire transient response of the driver interface (t_{rise}). The ideal emission signal (discounting fluorescence lifetime) is:

$$\text{output} = KI_{\text{ss}}T_{\text{int}} \quad (2)$$

where K is the scaling factor that converts the integrated signal to an output voltage, and I_{ss} is the emission signal from the fluorophore. When the effect of the response time (t_{rise}) of the driver interface is incorporated into the signal integrated by the photodetector, the total signal out becomes:

$$\text{output} = KI_{\text{ss}}(T_{\text{int}} - t_{\text{rise}}) \quad (3)$$

which results in an error of:

$$\text{error} = \frac{KI_{\text{ss}}T_{\text{int}} - KI_{\text{ss}}(T_{\text{int}} - t_{\text{rise}})}{KI_{\text{ss}}T_{\text{int}}} = \frac{t_{\text{rise}}}{T_{\text{int}}} \quad (4)$$

This analysis assumes that the integration time of the photodetector is less than the “on” cycle of the LED, thereby eliminating the impact of the fall time (decreasing transients) on the accuracy of the emission signal. Typical errors induced by the response time of the PCB-based implementation ($t_{\text{rise}} = 40$ ns) for several common photodetectors are:

- Photomultiplier tube (Hamamatsu #H7827-002): a 0.8% error (worst-case) at a maximum recommended operating frequency of 200 kHz;
- Avalanche photodiode (Hamamatsu S5345): a 3.2% error (worst-case) assuming a measurement time $10\times$ the maximum operating frequency of the APD;
- CCD (Hamamatsu S7010): a 0.67% error (worst-case) with a minimum integration time of 6 ms.

If the integration time spans multiple LED control pulses, the error incorporates the fall time as well:

$$\text{error} = \frac{t_{\text{rise}} + t_{\text{fall}}}{T_{\text{int}}} \quad (5)$$

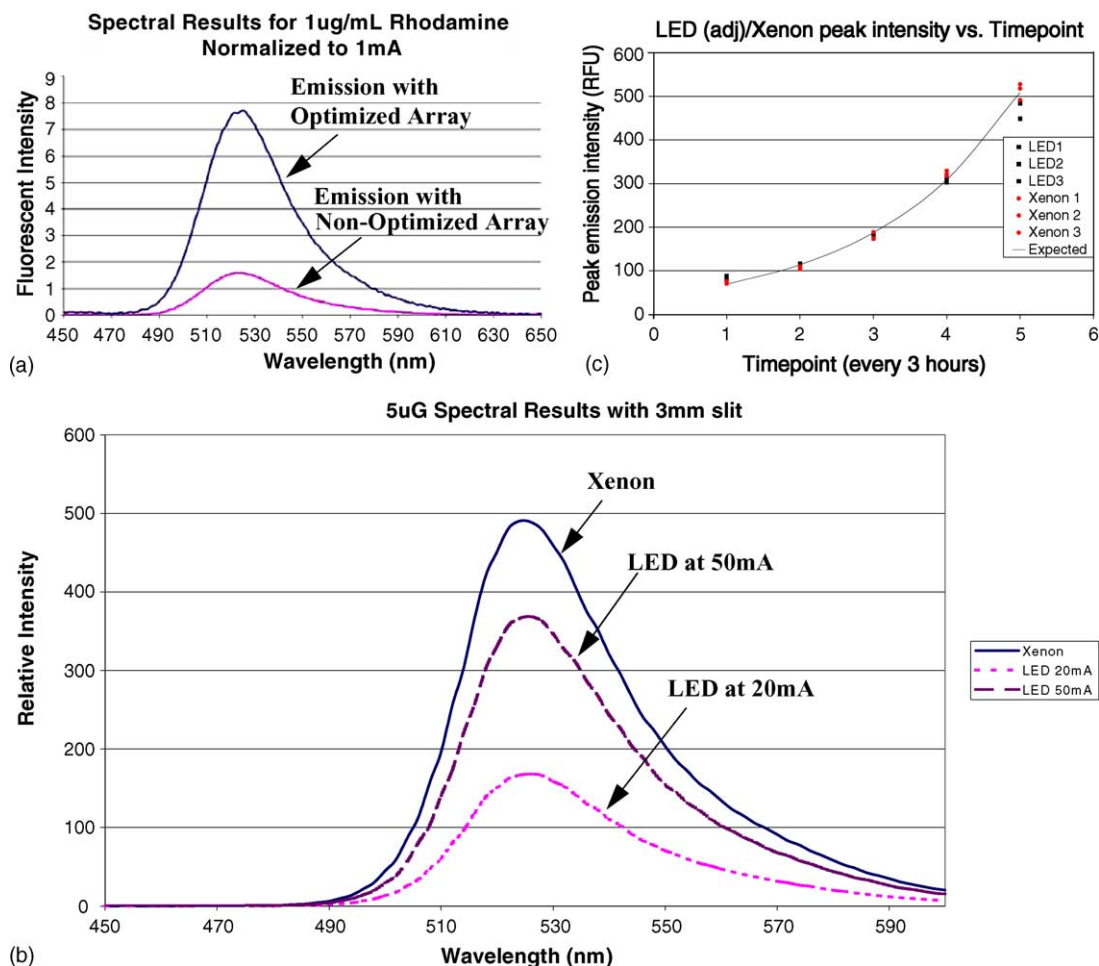


Fig. 9. System results. The viability of an LED array-based system, as described in this paper, has been evaluated for: (a) long-term experiments for monitoring AM1 bacteria growth and short-term experiments with (b) GFPuv tagged to AM1 *Methylobacterium extorquens* bacteria and (c) Rhodamine 123 dye.

In order to achieve suitability for fluorescence lifetime measurements, the response time of the input light source must be less than the lifetime of the fluorophore, so that once the fluorophore emits, the excitation light is no longer present in the output path. The maximum response time of the PCB-based (DIP package) implementation presented here is 40 ns, which is compatible with longer lifetime fluorophores (e.g. $[\text{Ru}(\text{bpy})_3]^{2+}$ with lifetime >100 ns [11]) phosphorescing agents (lifetimes on the order of ms and greater), and hybrid molecules that combine fluorescence and phosphorescence (lifetimes between microseconds and milliseconds). A surface mount implementation is expected to reduce the response time by an order of magnitude to 4 ns; an integrated implementation can reduce the response time even further to sub-ns level, but will require integrated LEDs in special packaging to reduce parasitic capacitance at the interface between the driver circuits and the LEDs.

6. System: results and discussion

Lifetime increases due to low duty cycle operation and spectral output stability allow LEDs to be overdriven to

achieve the power levels of conventional light sources in practical biological analysis experiments. The capability of the LED array, interface module, and system architecture to perform comparable to existing fluorimeters has been demonstrated in two short-term and one long-term experiments representative of typical fluorescence analysis. The two short-term experiments monitor the fluorescence intensity of: (a) GFPuv attached to AM1 *M. extorquens* bacteria and (b) Rhodamine 123 dye (Fig. 9a and b). In the GFPuv experiment, the overdriven LED array is shown to achieve comparable total emission signal to a conventional fluorometer using a xenon lamp. Results show that the LED excitation source is capable of producing an emission signal within 25% of the signal obtained, when using a xenon source (Fig. 9a). An array of five purple LEDs operating at 50 mA (overdrive operation) is used to obtain these results. The usefulness of both array and overdrive capabilities are demonstrated through this experiment. In the Rhodamine 123 experiment, the flexibility of the LED array and the associated optimization software clearly show that, when an array of LEDs is optimized to a particular fluorescing agent, higher emission signal and improved SNR performance is possible.

The LED interface module and system architecture is also demonstrated in longer term monitoring of AM1 *M. extroquens* bacteria growth to establish the comparable stability of the LED module to a xenon source. Results are shown in Fig. 9c. A 24-h growth study compares the emission signal generated over time by the LEDs to that of a conventional xenon excitation source. The results are comparable verifying that the stability of the LED approach is suitable to longer term fluorescence analysis systems.

These three system level experiments verify the usefulness of the LED interface module and system architecture for biological analysis, when fluorescing (or luminescing) agents are used.

7. Conclusion

This paper has presented a design framework for LED-based fluorescence analysis systems that enables significantly increased spectral flexibility and lifetime over other LED-based systems. LED-based systems show important improvements over conventional fluorometer designs that use white-light sources including improved portability (reduced cost, power, and size), increased modularity, and better spatial uniformity (lack of imaging artifacts). The system presented here includes an electronic interface capable of generating high power output from the LEDs without significant degradation in lifetime stability. Such an improvement in power output is absolutely necessary to make LED-based systems competitive with conventional fluorometers for general-purpose fluorescence analysis applications. The LED-array-based system here presents, up to a 93% improvement in stability over other LED-based systems, up to 100-fold increase in light output over single LED systems, and millions of possible combinations of spectral output (as compared to a 1–10 possible spectral outputs with one to two LED array-based systems demonstrated for fluorescence analysis). These benefits over previous LED-based systems are achieved at a reduction in power, space, and cost of at least one order of magnitude over conventional white-light source-based systems. Used in conjunction with appropriate optics, this electronic interface provides a highly competitive, portable (small footprint) alternative to conventional fluorometer designs. Future work will include the insertion of a feedback loop in the input (light source) and output (photodetection) loop to further improve stability and accuracy of an LED-based system.

References

- [1] J.R. Lakowicz, Principles of Fluorescence Spectroscopy, Kluwer Academic/Plenum Publishers, New York, 1999, pp. 28.
- [5] S. Dets, N. Denisov, Blue LED's feasibility for fluorescence analysis, in: Proceedings of SPIE, Optical Biopsy III, vol. 3917, San Jose, CA, 23–24 January 2000, pp. 130–138.
- [6] O.W. Liew, J.-W. Chen, A.K. Asundi, Development of fiber optic spectroscopy for in-vitro and in-plant detection of fluorescent proteins, in: Proceedings of the SPIE, vol. 4596, 2001, pp. 208–218.

- [7] L. Randers-Eichhorn, C.R. Albano, J. Sipiior, W.E. Bentley, G. Rao, On-line green fluorescent protein sensor with LED excitation, Biotechnol. Bioeng. 55 (6) (1994) 921–926.
- [8] S.-R. He, H.-F. Xu, Research on green LED as fluorescent excitation source, Optical Techn. 28 (1) (2002) 9–10.
- [9] S. Gao, X. Luo, X. Lan, Y. Liu, J. Lu, X. Ni, Analyzing of LED-induced blood fluorescent spectra, Chin. J. Lasers B 11 (4) (2002) 315–318.
- [10] A.G. Ryder, S. Power, T.J. Glynn, Evaluation of acridine in nafion as a fluorescence-lifetime-based pH sensor, Appl. Spectrosc. 57 (1) (2003) 73–79.
- [11] W.J. O'Hagen, M. McKenna, D.C. Sherington, O.J. Rolinski, D.J.S. Birch, MHz LED source for nanosecond fluorescence sensing, Meas. Sci. Technol. 13 (1) (2002) 84–91.
- [12] T.H. Jeys, L. Desmarais, E.J. Lynch, J.R. Ochoa, Development of a UV LED-based biosensor, in: Proceedings of SPIE, Sensor and Command, Control, Communications and intelligence Technologies for Homeland Defense and Law Enforcement II, vol. 5071, Orlando, FL, 21–25 April, 2003, pp. 234–240.
- [13] H. Szmazinski, Q. Chang, Micro and sub-nanosecond lifetime measurements using a UV light-emitting diode, Appl. Spectrosc. 54 (1) (2000) 106–109.
- [14] E.M. Rabinovich, M.J. O'Brien, A.A. Ukhonov, R.K. Jain, V.H. Perez-Luna, G.P. Lopez, Fluorescence lifetime-based phase-sensitive sensor array with LED or diode laser excitation for chemical and biosensing, in: Proceedings of SPIE, Biomedical Sensors, Fibers, and Optical Delivery Systems, Stockholm, Sweden, vol. 3570, 8–10 September, 1998, pp. 236–243.
- [15] J.A. Goldman, D.E. Sullivan, I. Kordunsky, Continuous fluorescence detection thermal cycling for DNA analysis using an array of LED light sources, in: Proceedings of SPIE, Biomedical Nanotechnology Architectures and Applications, 20–24 January, San Jose, CA, 2002, pp. 252–258.
- [16] Ocean Optics Inc. [Online]. Model USB-LS-450 LED Light Source. Available: <http://www.oceanoptics.com/products/usbls450.asp>. 10 September 2004 [date accessed].
- [17] Turner Designs Incorporated [Online]. Available: <http://www.turnerdesigns.com/t2/instruments/td700.html>, 2 September 2003 [date accessed].
- [18] N. Banani, L. Lee, M.R. Holl, B. Marquardt, M. Troll, D.M. Wilson, SLAP: design software for optimization of fluorescence analysis systems, in: IEEE Engineering in Medicine and Biology Conference, 1–5 September, San Francisco, CA, 2004.
- [19] BD Biosciences [Online]. New Living Colors GFP Vectors. Available: <http://www.bdbiosciences.com/clontech/archive/JUL96UPD/PDF/JUL96GFP.pdf>. 10 September 2004 [date accessed].
- [20] Molecular Probes [Online]. Spectral characteristics for Molecular Probes' dyes. Available: <http://www.probes.com/handbook/tables/0372.html>. 10 September 2004 [date accessed].

Biographies

Andrew Moe is a graduate student at the University of Washington in the U.S. He received his BS in electrical engineering from Seattle Pacific University in 2001. His research is in miniaturized fluorescence analysis instrumentation systems.

Steve Marx is a graduate student at the University of Washington in the U.S., with a BS in electrical engineering from Seattle Pacific University in 2001. His research interests are the design of ionic sensors using MOS-FET technology and miniaturized fluorescence analysis instrumentation systems.

Naureen Banani is a graduate student at the University of Washington in the U.S. She received her BS in electrical engineering from the Uni-

versity of Washington in 2004 with an emphasis in analog and digital signal processing. Her research is in optimization software for dynamic configuration of fluorescence excitation systems.

Shih-Hao (Matthew) Liu is an undergraduate at the University of Washington pursuing BS degrees in electrical engineering and computer engineering. His research interests emphasize process improvement and software simulation for efficient hardware development.

Denise Wilson is an associate professor at the University of Washington in the U.S. She received her PhD and MS in electrical engineering from the Georgia Institute of Technology in 1995 and 1989, respectively. She has a BS in mechanical engineering from Stanford University and has worked for several years for Applied Materials, a semiconductor capital equipment supplier from 1990 to 1992. Her research interests focus on the development of signal processing architectures, array platforms and other infrastructure for visual, auditory and chemical sensing microsystems.